

Sensor of small movements, based on one-dimensional photonic crystal with defect

© A.I. Sidorov¹, M.V. Mahaeva²

¹ ITMO University,
197101 St. Petersburg, Russia

² St. Petersburg State Electrotechnical University „LETI“,
197376 St. Petersburg, Russia

e-mail: sidorov@oi.ifmo.ru

Received April 14, 2023

Revised April 14, 2023

Accepted April 28, 2023

The results of computer simulation of optical properties of one-dimensional (1D) photonic crystal (PC) with defect, based on the layers Si-SiO₂ in near IR range are presented. The optical thicknesses of layers, which form PC, were $\lambda/4$, $3\lambda/4$ and $10\lambda/4$. Defect was formed by air gap in the middle of PC. The influence of defect thickness on spectral position of the transmission band of defect was studied. It was shown that the sensitivity on the defect thickness d is in the range of $\Delta\lambda/\Delta d = 330\text{--}1200\text{ nm}/\mu\text{m}$ and $0.6\text{--}0.85\text{ dB/nm}$, depending on sensor geometry and measurement method. This makes 1D PC with defect promising for the use as sensitive element in sensors of small movements.

Keywords: sensor of movements, photonic crystal, defect, photonic bandgap, transfer matrix.

DOI: 10.61011/EOS.2023.07.57136.4860-23

Introduction

Small displacement measurement plays an important role in high-tech industries. In particular, in the manufacture of liquid crystal displays (LCD) and in the manufacture of semiconductors. There are a number of small displacement sensors with high sensitivity. Optical displacement sensors provide high resolution. They have high sensitivity and are not sensitive to electromagnetic blasts. An example is a coherent photonic scanning tunneling microscope with a resolution of 1.6 nm [1]. It uses heterodyne interferometry to measure both the phase and amplitude of the optical short-range field. Another example is a homodyne polarization laser interferometer for high-speed small displacement measurements with a resolution of 0.5 nm [2]. The small displacement sensor described in [3], based on the critical angle method and the confocal method, has a resolution of approximately 5 nm. In [4] it is shown that using geometric optics and plasmon resonance in metal nanoparticles nanometer resolution is possible to be obtained when measuring absolute distances. Meanwhile, most small displacement sensors have a complex design and high cost.

PC and photonic crystal fibers are widely used in sensing [5–11]. PC and fibers are resonant optical systems. Their spectral and amplitude characteristics depend on external and internal changes, such as temperature, pressure, field-induced birefringence, and medium refraction index. All these effects can be used in the development of sensors. PC can be used to measure temperature [12], the medium refraction index [9], electric and magnetic fields, mechanical

stress, angles, including for measuring small displacements. In [13,14] small displacement sensors based on photonic crystal fibers are described. Metamaterials [15–17] can be used to create 1D PC.

If the periodicity of the photonic crystal is disrupted by a defect, then a specific spectral area with different optical properties can be created. The defect area can support modes with frequencies inside the photonic band gap. But since the defect guidance band is surrounded by a photonic band gap, emission within the defect remains limited. As a rule, the defect guidance band is very narrow. This allows the creation of sensors with very high sensitivity.

The purpose of this paper was to study the optical properties of a 1D PC with a defect from the point of view of the opportunity of its use as a small displacement sensor, as well as to consider the influence of the PC geometry on its sensitivity.

1. PC geometry and method of numeric simulation

1D PC consists of 4 pairs of Si-SiO₂ layers with a defect in the center, which is an air gap ($n = 1$). Si and SiO₂ layers have a high refraction index contrast: $n = 3.4$ and 1.46 , respectively. This allows the use of only 4 pairs of layers in a photonic crystal without deteriorating its optical characteristics. The layers can be formed by vacuum deposition on silicon wafers with a thickness of 1–2 mm. The outer surfaces of silicon wafers should have anti-reflective coatings. It should be noted that the internal surfaces of silicon wafers participate in interference

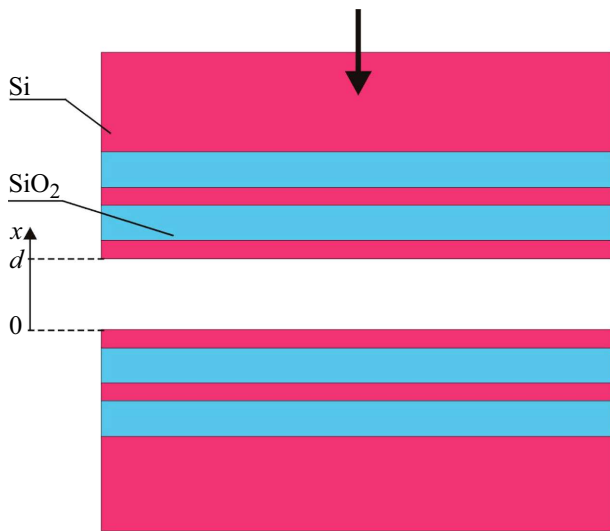


Figure 1. Geometry of PC with a defect.

processes in PC. Three PC geometries were used in the numerical simulation. In the first geometry, the optical thickness of the layers was equal to $\lambda/4$ for $\lambda = 1.5 \mu\text{m}$. In the second and third geometries, the optical thicknesses of the layers were equal to $3\lambda/4$ and $10\lambda/4$, respectively. The thickness of the defect is chosen so that the photonic band gap is located near the wavelength $1.5 \mu\text{m}$.

To measure displacements, one half of the PC is fixed inactive, and the second is mounted on a displacing object. The thickness of the defect changes at the displacement of the object. Since a change in the thickness of a defect leads to a spectral shift in the PC defect guidance band, the spectral shift in the defect guidance band can be used to measure displacement. For these purposes a spectrophotometer can be used. However, to increase the sensitivity and to reduce the dimensions of the sensor measuring part, it is preferable to use a narrow-band tunable semiconductor DFB (Distributed Feedback) laser as a radiation source. In this case a photodiode can be used as a photodetector. The second method is based on measuring the transmittance of a photonic crystal at a fixed wavelength corresponding to the wavelength of the probing laser.

It is obvious that a photonic crystal with the geometry shown in Fig. 1 can be considered as a multilayer interferometer. Therefore, the transfer matrix method [18] was used to simulate its optical properties. In this method the field amplitudes at the input (E_{j-1}) and output (E_j) of the layers boundaries are generally described by the following matrices:

$$\begin{bmatrix} E_{(j-1)-}^t \\ E_{(j-1)-}^r \end{bmatrix} = M_j \begin{bmatrix} E_{j-}^r \\ E_{j-}^t \end{bmatrix}, \quad (1)$$

$$M_j = \begin{bmatrix} \frac{\exp(i\theta_j)}{g_{j-1}} & \frac{f_{j-1}}{g_{j-1}} \exp(-i\theta_j) \\ \frac{f_{j-1}}{g_{j-1}} \exp(i\theta_j) & \frac{\exp(-i\theta_j)}{g_{j-1}} \end{bmatrix}. \quad (2)$$

Here the index „-“ corresponds to the reflected wave, t and r correspond to the transverse and radial components

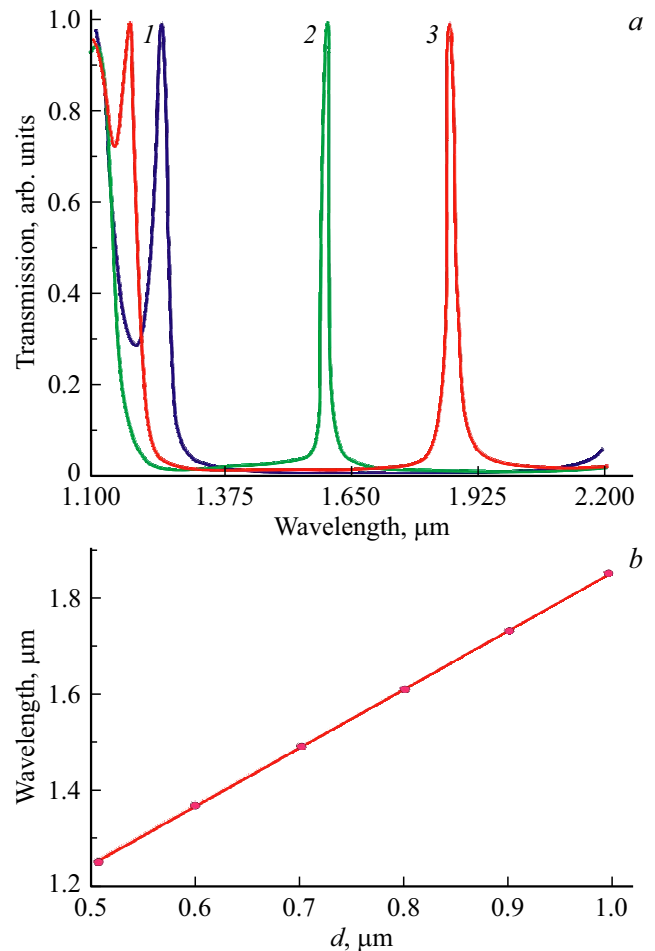


Figure 2. a — spectrum of part of the photonic band gap of a PC with a defect. The optical thickness of the PC layers is $\lambda/4$. $d = 0.5$ (1), 0.7 (2), $0.8 \mu\text{m}$ (3). b — the dependence of the spectral position of the maximum of the defect guidance band on the thickness of the defect.

of the wave, f and g — Fresnel coefficients:

$$f_{j-1} = \frac{n_{j-1} - n_j}{n_{j-1} + n_j}, \quad g_{j-1} = \frac{2n_{j-1}}{n_{j-1} + n_j}. \quad (3)$$

The transfer matrix is defined by the following expression:

$$M = \prod_{j=1}^{m-1} M_j, \quad (4)$$

where m — the number of layers.

The simulation used the dispersion of the optical constants of Si and SiO₂ from [19]. Absorption in FC was not taken into account. The simulation was carried out for normal radiation incidence in the Mathcad 15 environment.

2. Results and discussion

Figure 2, a shows the photonic band gap of a PC with a defect for various defect thicknesses for a PC with an

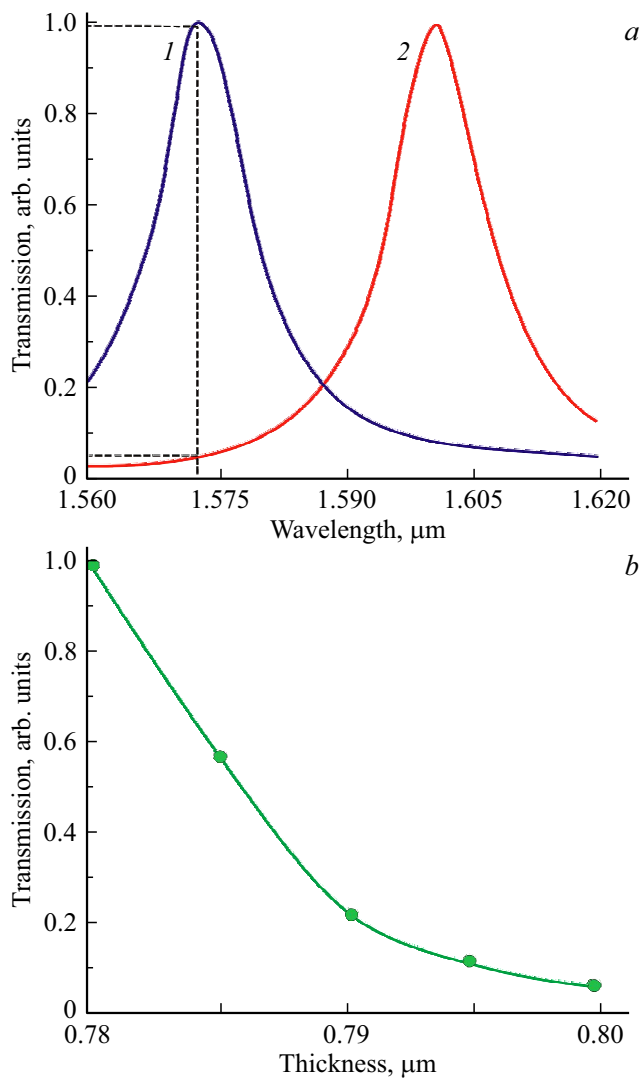


Figure 3. *a* — the spectral position of the defect guidance band at different defect thicknesses and the measurement technique at a fixed wavelength. $d = 0.78$ (1), $0.8 \mu\text{m}$ (2). *b* — the dependence of PC transmittance on defect thickness when measured at a fixed wavelength $\lambda = 1.574 \mu\text{m}$ (marked with a dashed line in Fig. 3, *a*). The optical thickness of the PC layers is $\lambda/4$.

optical layer thickness equal to $\lambda/4$. The band gap is approximately equal to $1 \mu\text{m}$. The width at half maximum of the defect guidance band is 8 nm. Increasing the thickness of the defect leads to a long-wavelength shift of the defect guidance band and a decrease in the band gap. It can be seen from the figure that a decrease in the band gap affects mainly the spectral shift of the short-wavelength part of the band gap. This effect also affects the spectral shift of the defect guidance band. Figure 2, *b* shows the dependence of the spectral position of the maximum of the defect guidance band on the thickness of the defect. It can be seen from the figure that the dependence is linear, and the spectral sensitivity of measurements with an optical thickness of PC layers equal to $\lambda/4$ is $\Delta\lambda/\Delta d = 1200 \text{ nm}/\mu\text{m}$.

Fig. 3, *a* shows the spectral position of the defect guidance band at different defect thicknesses and the measurement technique at a fixed wavelength. It can be seen from the figure that as the thickness of the defect increases, a long-wavelength shift of the defect band occurs. Meanwhile, at the wavelength corresponding to the maximum defect guidance band at its original thickness, the transmission decreases. Figure 3, *b* shows the dependence of the photonic crystal transmission on the defect thickness when measured at a fixed wavelength. As can be seen from the figure, with a small change in the thickness of the defect, the dependence is close to linear. As the thickness increases, the dependence becomes flatter. The average amplitude sensitivity of measurements by this method with an optical thickness of PC layers equal to $\lambda/4$ is 0.61 dB/nm.

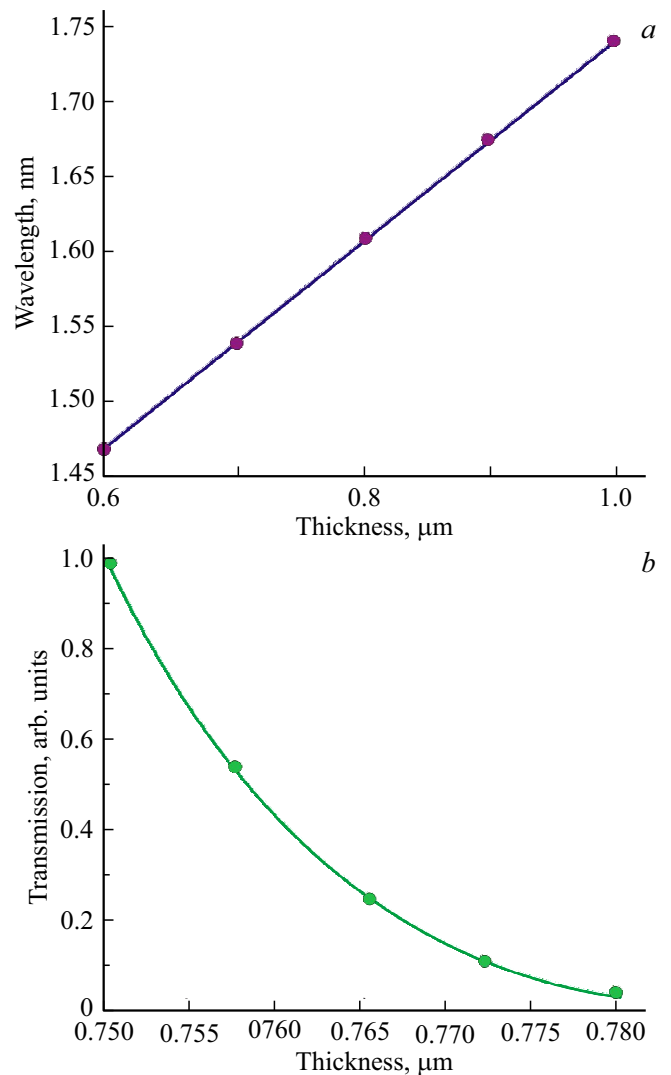


Figure 4. *a* — spectral position of the defect transmission guidance band at $d = 0.78$ (1), $0.8 \mu\text{m}$ (2). *b* — dependence of PC transmission on defect thickness when measured at a fixed wavelength $\lambda = 1.562 \mu\text{m}$. The optical thickness of the PC layers is $3\lambda/4$.

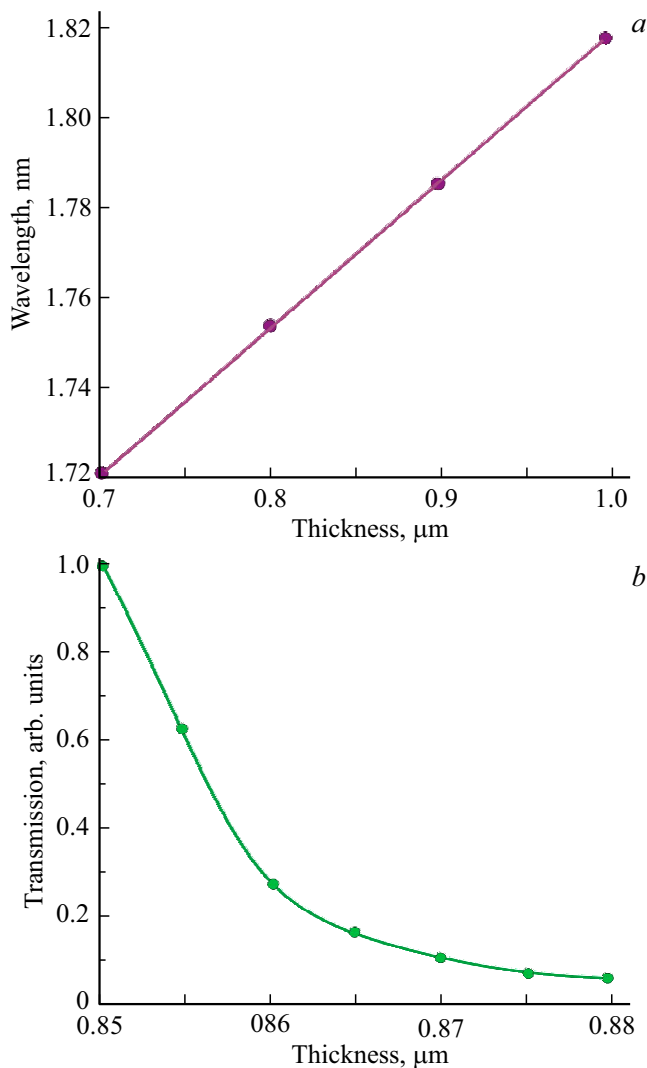


Figure 5. Dependences of the spectral position of the defect guidance band maximum (a) and PC transmittance at a fixed wavelength $\lambda = 1.766 \mu\text{m}$ (b) on the defect thickness. The optical thickness of the PC layers is $10\lambda/4$.

As the optical thickness of the PC layers increases from $\lambda/4$ to $3\lambda/4$, the spectral width of the PC photonic band gap decreases and the spectral defect guidance band decreases. The first factor leads to a decrease in the dynamic range of measurements. The second factor — to increase the amplitude sensitivity of measurements at a fixed wavelength. Figure 4 shows the spectral position of the defect guidance band for different defect thicknesses and the dependence of the PC transmittance on the defect thickness when measured at a fixed wavelength for the optical thickness of the PC layers equal to $3\lambda/4$. The spectral sensitivity of measurements with an optical thickness of PC layers equal to $3\lambda/4$ is $780 \text{ nm}/\mu\text{m}$. The average amplitude sensitivity of measurements, in this case, is equal to $0.76 \text{ dB}/\text{nm}$.

As the optical thickness of the PC layers increases further up to $10\lambda/4$, the spectral width of the PC photonic band gap decreases and the spectral defect guidance band decreases. As in the previous case, the first factor leads to a decrease in the dynamic range of measurements. The second factor — to increase the amplitude sensitivity of measurements at a fixed wavelength. In addition, the PC has several band gaps. This simplifies the selection of the operating wavelength. In addition, this allows to carry out measurements at several wavelengths simultaneously. Figure 5 shows the spectral position of the defect guidance band for different defect thicknesses and the dependence of the PC transmittance on the defect thickness when measured at a fixed wavelength for the optical thickness of the PC layers equal to $10\lambda/4$. The spectral sensitivity of measurements is $327 \text{ nm}/\mu\text{m}$. The average amplitude sensitivity of measurements, in this case, is equal to $0.85 \text{ dB}/\text{nm}$.

Thus, an increase in the optical thickness of PC layers leads to a decrease in the spectral sensitivity of measurements, but is accompanied by an increase in the sensitivity of amplitude measurements.

Conclusion

Numerical modeling of the optical properties of a 1D photonic crystal with a defect, consisting of layers of silicon and silicon oxide and a defect in the form of an air gap, showed that such a photonic crystal can be used as a small displacement sensor. The effect is based on the spectral shift of the defect's transmission band as the thickness of the defect changes. The maximum sensitivity when measuring the spectral shift is $1200 \text{ nm}/\mu\text{m}$ for a photonic crystal with an optical layer thickness of $\lambda/4$. The maximum sensitivity when measuring at a fixed wavelength is $0.85 \text{ dB}/\text{nm}$ for a photonic crystal with optical layer thickness $10\lambda/4$. The sensor can operate in both transmittance and reflection modes. The sensing element can be located at a distance from the measuring part of the sensor.

Funding

This study was performed as part of the Program „Priority 2030“.

Conflict of interest

The authors declare that they have no conflict of interest.

References

- [1] A. Nesci, R. Dändliker, H.P. Herzig. *Opt. Lett.*, **26**, 208 (2001). DOI: 10.1364/ol.26.000208
- [2] X. Liu, W. Clegg, D.F.L. Jenkins, B. Liu. *IEEE Trans. Instrum. Meas.*, **50**, 868 (2001). DOI: 10.1109/19.948290
- [3] S.J. Liao, S.F. Wang, M.H. Chiu. *SPIE*, **5635**, 211 (2005). DOI: 10.1117/12.572739

- [4] M.H. Chiu, B.Y. Shih, C.W. Lai, L.H. Shyu, T.H. Wu. *Sens. Act. A*, **141**, 217 (2008). DOI: 10.1364/AO.54.002885
- [5] J.B. Markowski. *ES 530B: Res. Proj.*, Hindawi Publ. Corp., 17, 535 (2008).
- [6] A.M.R. Pinto, M. Lopez-Amo. *J. Sens.*, **2012**, 598178 (2012). DOI: 10.1155/2012/598178
- [7] S. Upadhyay, V.L. Kalyan. *Intern. J. Eng. Res. Techn.*, **4**, 1006 (2015). DOI: 10.1007/s11468-019-00934-9
- [8] Z. Baraket, J. Zaghdoudi, M. Kanzari. *Opt. Mater.*, **64**, 147 (2017). DOI: 10.1016/J.OPTMAT.2016.12.005
- [9] A.I. Sidorov, L.A. Ignatieva. *Optik*, **245**, 167685 (2021). DOI: 10.1016/j.ijleo.2021
- [10] E. Chow, A. Grot, L.W. Mirkarimi, M. Sigalas, G. Girolami. *Opt. Lett.*, **29**, 1093 (2004). DOI: 10.1364/OL.29.001093
- [11] W.C.L. Hopman, P. Pottier, D. Yudistira, J. van Lith, P.V. Lambeck, R.M. de la Rue, A. Driessen, H.J.W.M. Hoekstra, R.M. de Ridder. *IEEE J. Sel. Top. Quant. Electron.*, **11**, 11 (2005). DOI: 10.1109/JSTQE.2004.841693
- [12] A.I. Sidorov, Yu.O. Vidimina. *Opt. Spectrosc.*, **130** (9), 158 (2022).
- [13] A.M.R. Pinto, J.M. Baptista, J.L. Santos, M. Lopez-Amo, O. Frazão. *Fiber Sensors*, **12**, 17497 (2012). DOI: 10.3390/s121217497
- [14] J.N. Dash, R. Jha, J. Villatoro, S. Dass. *Opt. Lett.*, **40**, 467 (2015). DOI: 10.1364/OL.40.000467
- [15] H. Wang, S. Chen, S. Zhu. *Phys. Rev. B*, **70**, 245102 (2004). DOI: 10.1103/PhysRevB.70.245102
- [16] H. Jiang, H. Chen, H. Li, Y. Zhang, J. Zi, S. Zhu. *Phys. Rev. E*, **69**, 066607 (2004). DOI: 10.1103/PhysRevE.69.066607
- [17] F. Wu, T. Liu, M. Chen, S. Xiao. *Opt. Expr.*, **30**, 33911 (2022). DOI: 10.1364/OE.469368
- [18] M. Born, E. Wolf. *Principles of optics: electromagnetic theory of propagation, interference and diffraction of light* (Cambridge University, 2000).
- [19] E.D. Palik. *Handbook of optical constants of solids* (Academic press, San Diego, 1998), v. 3.

Translated by E.Potapova